Desalination and Water Treatment
www.deswater.com

doi: 10.5004/dwt.2021.27797

241 (2021) 340–349
November

A modified first-order vegetation model for soil moisture retrieval in wheat fields using Sentinel-1 data

Yan Li[a,b], Chengcai Zhang[a,*], Weidong Heng[a], Feng Yang[c], Jisheng Liu[c]

[a]*School of Water Conservancy Science & Engineering, Zhengzhou University, Zhengzhou 450001, China, email: 1459567002@qq.com (C. Zhang)*
[b]*Zhengzhou Vocational College of Industrial Safety, Zhengzhou 451192, China*
[c]*Chushandian Reservoir Management Bureau, Xinyang 464000, China*

Received 17 August 2021; Accepted 23 September 2021

ABSTRACT

Soil moisture is an important factor affecting crop growth. In our work, the aim of this paper is to retrieve volumetric soil moisture in wheat fields using Sentinel-1 synthetic aperture radar (SAR) data. In order to eliminate the effect of wheat cover, we used a first-order vegetation model and improved the model. Then the support vector regression technique was used to retrieve soil moisture and validate the performance using experimental data. Three experimental campaigns were conducted in the Hebi, Northeastern Henan in different periods of wheat growth in 2019, with simultaneous satellite overpass. Compared with the water cloud model, the retrieved soil moisture given by the modified first-order vegetation model agreed better with field measurements, the R^2 and root mean square error value of this modified first-order vegetation model was (0.847, 0.015), (0.901, 0.016) and (0.936, 0.014) for the three experiments respectively. The results show that the modified first-order vegetation model based on the Sentinel-1 SAR data satisfied the requirement of soil moisture retrieval in the study region.

Keywords: Soil moisture; Sentinel-1 data; First-order vegetation model; Support vector regression

1. Introduction

Soil moisture (SM) is a key variable that couples the land and the atmosphere, and the energy and water cycles. It plays an essential role in hydrology, climatology, meteorology, ecology, and agronomy [1]. SM is especially important in arid or semi-arid agricultural regions, where its spatio-temporal distribution affects crop growth and development [2]. Despite its importance, it is difficult to accurately retrieve SM over large scales, due to the complexity of natural surfaces (i.e., terrain roughness, large spatial heterogeneity, and the presence of vegetation) [3].

In recent decades, several quantitative studies have proven that microwave remote sensing, especially synthetic aperture radar (SAR), can effectively retrieve soil moisture [4,5]. As active instruments, SAR sensors provide soil moisture observations over large areas in all weather conditions during both the day and night [6,7]. Important SAR satellites include the European Space Agency (ESA)'s ERS-1/2, ENVISAT-1, and Sentinel-1; the Canadian Space Agency (CSA)'s Radarsat-1/2; the German Aerospace Center (DLR)'s TerraSAR-X, China's GF3, and Japan's ALOS-2. Sentinel-1 is an earth observation satellite that is part of global monitoring for the environment and security. It provides more channels for observing soil moisture at a high spatial resolution (10 m). Furthermore, it has a regular temporal coverage (6 d), and its data is freely available [8,9].

Retrieving SM with microwave remote sensing has been explored for more than 30 y, and has been established many theoretical models [10–13]. In addition, there are experience

* Corresponding author.

and semi-empirical models [14,15]. However, these models are generally applicable only for monitoring or retrieving SM in bare soil and sparsely vegetated areas, and in vegetated areas, the accuracy of these models is significantly reduced [16].

In order to solve the problem, numerous methods have been proposed [17–27]. Taking crops as the research object, Attema and Ulaby [17] proposed the water cloud model (WCM). In this model, the total backscattering can be simply described as the scattering reflected from vegetation canopy and the backscattering from the ground. Xun et al. [18] estimated SM from C-band Radarsat-2 SAR data by using the WCM to fit the Dubois model [19] to study the grassland vegetation area of the Northeastern Tibetan Plateau. Lin et al. [20] developed the WCM by using a Microwave Polarization Difference Index (MPDI) to express vegetation water content; they concluded that VV polarization is based on Sentinel-1A data, when combined with MPDI, could achieve the high retrieval accuracy for soil moisture. For ignoring the multiple scattering between the vegetation and the ground, the WCM is not applicable to some crops covered (e.g., with a certain height of corn, wheat, etc.). According to the characteristics of microwave scattering, the Michigan Microwave Canopy Scattering (MIMICS) describes the vegetation structure in detail [21]. Jiang et al. [22] combined the MIMICS and Advanced Integral Equation Model (AIEM) model to simulate the backscattering coefficient. Roo et al. [23] simplified the MIMICS model by removing the scattering layer between the vegetation stem and the ground surface. However, the parameters of the Roo Model were still complex. Aiming at retrieving SM conveniently and accurately, a first-order vegetation model was proposed by Shi et al. [24], which could accurately describe various backscattering mechanisms of crop-covered fields. Liu et al. [25], retrieved SM based on a first-order vegetation model. With two repeat pass SAR data, the vegetation effects were eliminated from the first-order vegetation model by the decomposition technology. However, the decomposition technology was based on the full polarization data. Once the radar data is single-polarization or multi-polarization data, it is not applicable.

Considering the above facts, the main aim of this study was to evaluate the use of Sentinel-1 SAR data to retrieve SM over wheat-covered areas, with a focus on the methodology for eliminating the influence of vegetation from the radar backscattering. To this end, a first-order vegetation model was used and modified. The vegetation index obtained from Sentinel-2 was used to express the vegetation fraction, which was an important parameter of the modified first-order vegetation model. Moreover, the support vector regression (SVR) technique [26,27], which has good robustness to the limited availability of reference results in various application domains, was applied to retrieve soil moisture information.

2. Study area and data

2.1. Study area

The study site chosen for this study was Hebi (113°59′E–114°45′E, 35°26′N–36°02′N), which is located in the North of Henan Province, China (Fig. 1). The agricultural fields analyzed in this study area mainly lie on the Huang-Huai-Hai Plain, which has a homogeneous soil texture. Dry spells occur between November and March, so the climate's seasonal characteristics are favorable for crop farming. The cropping systems in this area usually involve wheat, corn, cotton, and canola, and wheat cycles occur between late September (emergence) and middle June (harvest) of the following year. A total of 28 sampling sites were selected, on slopes between 0% and 5% (Fig. 1c).

2.2. Data

Three C-band Sentinel-1 SAR images of Hebi, Henan Province, China, acquired from March to May 2019, were used in this study. The spatial resolution of these interferometric wide (IW) images was 5 m × 20 m, with incidence angles between 29 and 46. For the purpose of retrieval, image preprocessing were based on the Sentinel Application Platform (SNAP) software. The process mainly involved radiometric calibration, image mosaics, geometric correction, and speckle noise removal. Fig. 2a shows the preprocessing results of Sentinel-1 SAR data of the study area on 9 April, 2019.

Three optical images, which had either no or few clouds, were acquired by Sentinel-2A over the study sites with the SAR data contemporaneous. These acquired optical images were level-2A data, which bottom-of-atmosphere reflectance had been corrected in cartographic geometry. We just need to resample to 10 m. Fig. 2b shows the Sentinel-2 data of the study area on 3 April, 2019.

Simultaneously with the Sentinel-1A acquisitions, four in situ measurements of soil moisture and vegetation were conducted. A total of 84 soil moisture samples were obtained over depths of 0–10 cm. For each sampling site, three sampling points were selected; the distance between each sampling point was approximately 10 m. The locations were recorded by the global positioning system (GPS) device. These gravimetric measurements were converted into volumetric moisture based on bulk density [28–32].

3. Math

Here, a proper SM retrieval method is proposed for wheat-covered fields. A flowchart of the processing steps for SM estimation is illustrated in Fig. 3. The SM retrieval method used here comprised three main phases. The first phase was obtaining parameters of the model from remote sensing. The second phase was the central part of the processing chain. The first-order vegetation model and SVR were implemented for SM retrieval in this region. Finally, the coefficient of determination (R^2) and root mean square error (RMSE) were calculated to evaluate the accuracy of the SM estimations, and the SM values were mapped across the study area. More details on each part of the soil moisture retrieval algorithm are given in Fig. 3.

3.1. First-order vegetation model

Vegetation canopies reduce the sensitivity of radar measurements to SM, thus affecting the accuracy of SM retrieval. Tackling this issue was the main aim of this study. According

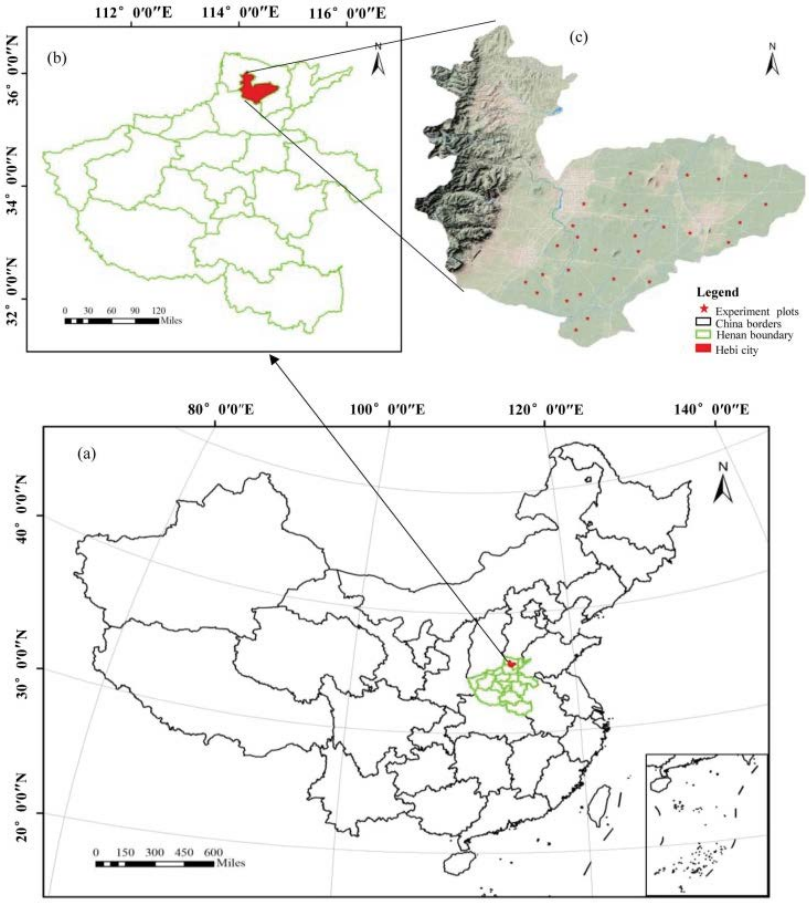

Fig. 1. General overview of the study area and map showing locations of sampling sites.

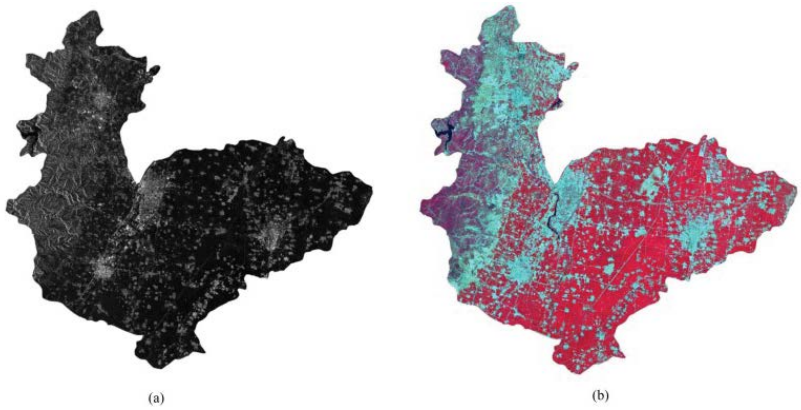

Fig. 2. Remote sensing images of the study area. (a) Sentinel-1 SAR image (VV polarization) and (b) Sentinel-2 composite false red green blue (RGB) images (Band 8 = red; Band 4 = green; Band 3 = blue).

to the first-order vegetation model, the total backscattering term over the vegetated fields can be decomposed into three parts: volume scattering in the canopy (Fig. 4a), surface scattering by the underlying ground surface (Fig. 4b), and multiple interactions involving both the canopy volume and the ground surface (Fig. 4c). To better describe the backscattering coefficients of the soil and vegetation in different periods of wheat-covered areas, the vegetation fraction was introduced into the model. For a given incidence angle, the model is described as follows:

$$\sigma_t^0 = f_v\sigma_v^0 + f_v\sigma_{sv}^0 + f_v\sigma_s^0 L^2 + \left(1 - f_v\right)\sigma_s^0 \quad (1)$$

where θ is the incident angle, f_v is the vegetation fraction, σ_t^0 is the total backscattering coefficient, σ_{veg}^0 is the backscatter contribution of the vegetation canopy, σ_{vs}^0 is the

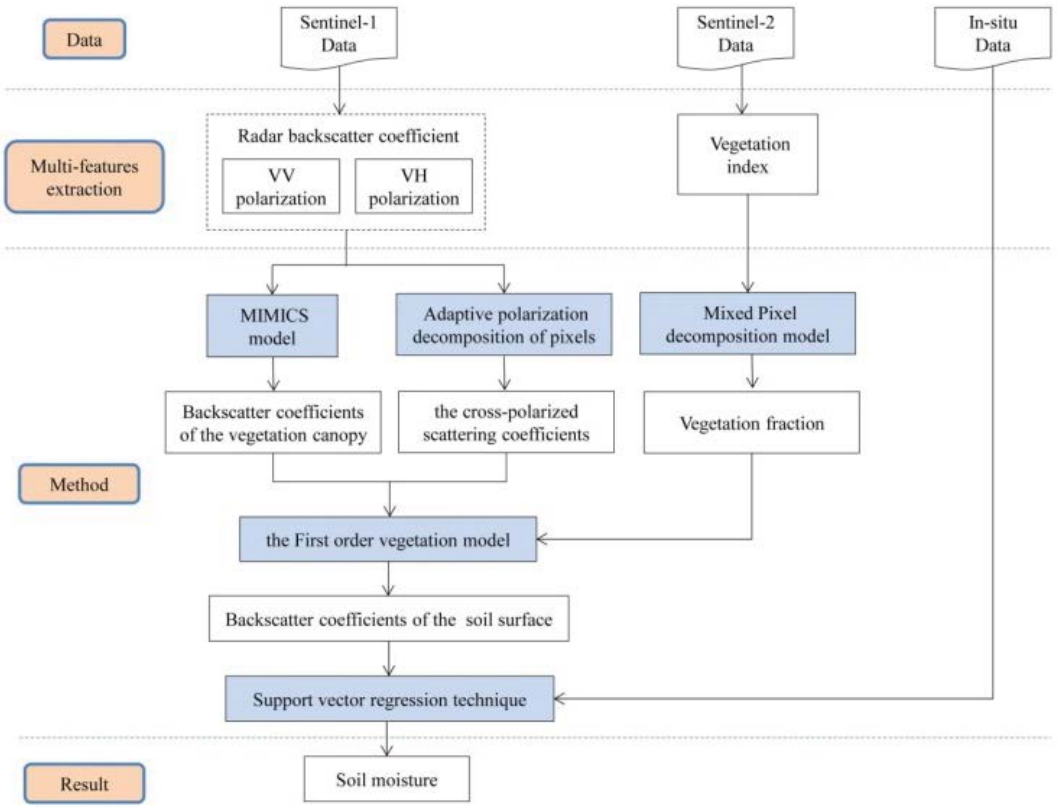

Fig. 3. Flowchart of the soil moisture retrieval process.

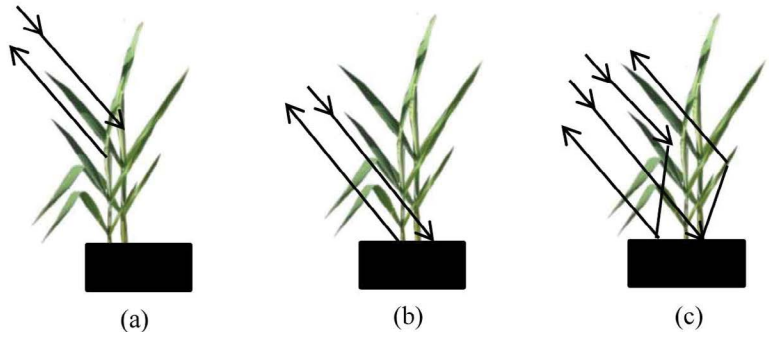

Fig. 4. Backscattering from wheat fields. (a) Volume scattering in the canopy, (b) surface scattering by the underlying ground surface, and (c) multiple interactions involving both the canopy volume and the ground surface.

cross-polarized scattering coefficients between vegetation and soil surface, σ^0_{soil} is the backscatter contribution of the soil surface, and L^2 is the double attenuation factor.

Based on the MIMICS model, the σ^0_{veg} can be expressed:

$$\sigma^0_v = \frac{\sigma_1 \cos\theta}{2k_e}\left(1 - L^2\right) \tag{2}$$

$$L^2 = \exp\left(-2\tau\sec\theta\right) \tag{3}$$

where σ_1 is the radar backscatter cross-section of leaves and stems in a unit volume of vegetation canopy, k_e is the canopy.

3.1.1. Extinction coefficient

In order to better reflect the growth characteristics of wheat, τ is expressed by the height of wheat (h) and the canopy extinction coefficient (k_e):

$$\tau = k_e \times h \tag{4}$$

Moreover, f_v is an additional parameter of first-order vegetation model; it is used to distinguish the proportion of vegetation coverage and bare soil in pixels. f_v can be calculated using the mixed pixel decomposition model [33]:

$$f_v = \frac{\left(\mathrm{NDVI} - NDVI_{\min}\right)}{\left(\mathrm{NDVI}_{\max} - \mathrm{NDVI}_{\min}\right)} \quad (5)$$

where $\mathrm{NDVI}_{\min}$ denotes the bare soil pixel, which is theoretically close to zero, and $\mathrm{NDVI}_{\max}$ denotes the pure vegetation pixel, which is theoretically close to one. In order to reduce the influence of weather conditions, a 0.5% confidence level was used to obtain the thresholds of $\mathrm{NDVI}_{\min}$ and $\mathrm{NDVI}_{\max}$.

It can be seen from the above analysis, the multiple scattering was difficult to solve in soil moisture retrieval. To overcome this difficulty, a polarization decomposition method based on the relationship between adjacent pixels was proposed as the acquisition mode in this study. As shown in Fig. 5a, assuming that in the neighborhood space of a certain pixel $P_{i,j}$ in the study area, the cross-scattering coefficient between vegetation and the ground surface (σ^0_{sv}), and the soil scattering coefficient (σ^0_{soil}) in each pixel are constant in each pixel. Then in this local space, the known parameters are brought into the Eq. (10) according to the different vegetation fraction (f_v) and the canopy extinction coefficient (k_e) corresponding to different pixels, and it is proposed to generate radar backscatter with different correlation functions $\sigma^0_c = f(\sigma^0_{sv}, \sigma^0_s)$ in the group. In this small space, a set of optimal solutions is assigned to the central pixel P_1 by using the least-squares method, and the soil backscattering coefficient of the pixel P_1 is obtained. Moving the center pixel to $P_{i,j+1}$, as shown in Fig. 5b, the soil backscattering coefficient of Pixel $P_{i,j+1}$ is obtained by the above method. By analogy, the backscattering coefficient of soil in the entire study area could be obtained.

3.2. SM retrieval

To achieve an efficient and robust SM retrieval algorithm, a machine learning technique, namely SVR was used. In detail, an SVR technique was applied that allowed for non-linear relationships between a target variable and several input features. The entire procedure was divided into two main phases: training and validation. For the 28 samples that were acquired in each period, 20 random samples were used for training and the rest were used for validation. Owing to its accurate estimation, good intrinsic generalization ability and ability to deal with complex nonlinear problems, the SVR technique can be widely applied for soil moisture estimation [34–36].

SVR is a supervised regression technique that transforms the nonlinear problem of the soil backscattering coefficient, normalized red edge index, vegetation coverage, and soil moisture into the linear problem of a higher dimensionality space, as follows:

$$f(x) = \sum_{i=1}^{n}\left(a_i - a_i^*\right)K\left(x_i, x\right) + b \quad (6)$$

where n is the number of training samples, a_i^* represents the Lagrange multipliers of the optimization problem, $k(\ldots)$ is a kernel function, x_i and x are the predictor variables, and b is the bias.

According to functional theory, kernel function can be used to construct a support vector machine. The commonly adopted kernel is the Gaussian Radial Basis Function (RBF) kernel. The RBF kernel has good anti-interference ability and less numerical difficulties than other kernel functions [37]. It can deal with samples when the relationship between class labels and features is nonlinear:

$$K(x, y) = \exp\left(-\frac{x - y^2}{2'^2}\right), \delta > 0 \quad (7)$$

where δ is the reach rate, that is, the rate at which soil moisture falls to 0.

4. Results and discussion

4.1. Estimation of backscattering coefficient of soil

In order to evaluate the effect of vegetation scattering on radar backscattering, different models are used to

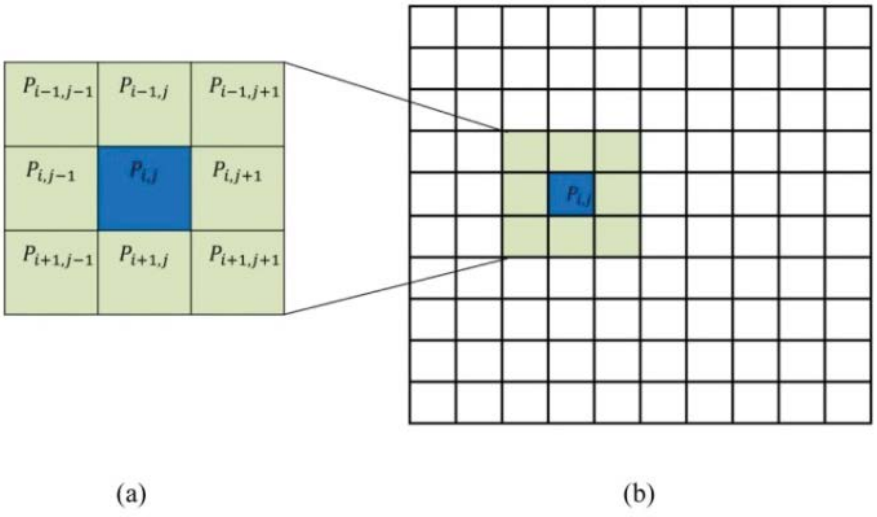

Fig. 5. The polarization decomposition method.

simulate (Fig. 6). Comparing the simulation results from the water cloud model and the modified first-order vegetation model, the correlation between the backscattering coefficient of soil and the radar backscattering coefficient is relatively divergent. A possible reason for this result is that the scattering effect of vegetation is further eliminated in the modified first-order vegetation model, and the relationship between soil scattering and radar scattering is reduced accordingly [38,39].

4.2. Retrieval of soil moisture

In order to evaluate the accuracy of the modified first-order vegetation model, three validation experiments were conducted for soil moisture retrieval. In each experiment, 20 random in-situ measured soil volumetric moisture was used for training, and another 8 was employed to calculate the R^2 and RMSE of the estimated SM. The relationships between the retrieved SM and the in-situ measurements are shown in Fig. 7, and the R^2 and RMSE values are summarized in Table 1. As seen in Fig. 7, there was a good linear relationship between the retrieved SM and the in-situ measurements at different growth stages of wheat. Moreover, the scattered points of the VV polarization were closer to the 1:1 line than that of VH polarization. As seen from Fig. 7a and b, the validation volumetric SM of the 8 sites were mainly distributed from 0.2 to 0.3 cm^3/cm^3, which is consistent with the in-situ measurement data. As seen from Fig. 7c–f, it was similar results from the in-situ measurement data, which showed the soil moisture of 8 sites was mainly from 0.2 to 0.4 cm^3/cm^3.

As seen in Table 1, on April 9, 2019, when wheat was in the jointing stage, the coefficient of determination R^2 and RMSE of retrieval volumetric SM based on the improved first-order vegetation model for VV polarization were 0.847 and 0.015 (Fig. 7a), while R^2 and RMSE values of the VH polarization were 0.688 and 0.015 (Fig. 7b). On May 3, 2019, when wheat was in the heading stage, the R^2 and RMSE values of the VV polarization were 0.901 and 0.016 (Fig. 7c), while the R^2 and RMSE values of the VH polarization were 0.768 and 0.019 (Fig. 7d). On May 23, 2019, when wheat was in the filling stage, R^2 and RMSE values of the improved first-order vegetation model for VV polarization were 0.936 and 0.014 (Fig. 7e), while 0.759 and 0.017 for VH polarization (Fig. 7f). Compared with the WCM, the retrieval of volumetric SM based on the improved first-order vegetation model agrees better with field measurements.

According to the retrieved results, VV polarization had good accuracy and stability for retrieval SM in the study area, and improved first-order vegetation model presented satisfactory results in retrieval SM with Sentinel-1 SAR data [40].

The study area SM maps are illustrated in Fig. 8. Based on the supervised classification technology of threshold segmentation by the Environment for Visualizing Images (ENVI) software, the non-wheat areas, such as towns, rivers and other non-agricultural areas in the Sentinel-1 SAR image of the study area were removed.

Fig. 8 demonstrates that SM in April, 2019 was relatively lower than in May 2019, and in May 2019, the SM was from 20% to 50% in most of the study area. The frequency distributions of the soil moisture retrieval results of these three times were basically consistent with the measured values on each period. This modified model therefore had strong applicability for the study area.

5. Conclusions

Taking Hebi, a representative area of wheat planting in Henan Province, as a study area, here the potential of C-band Sentinel-1 SAR data for SM retrieval was investigated

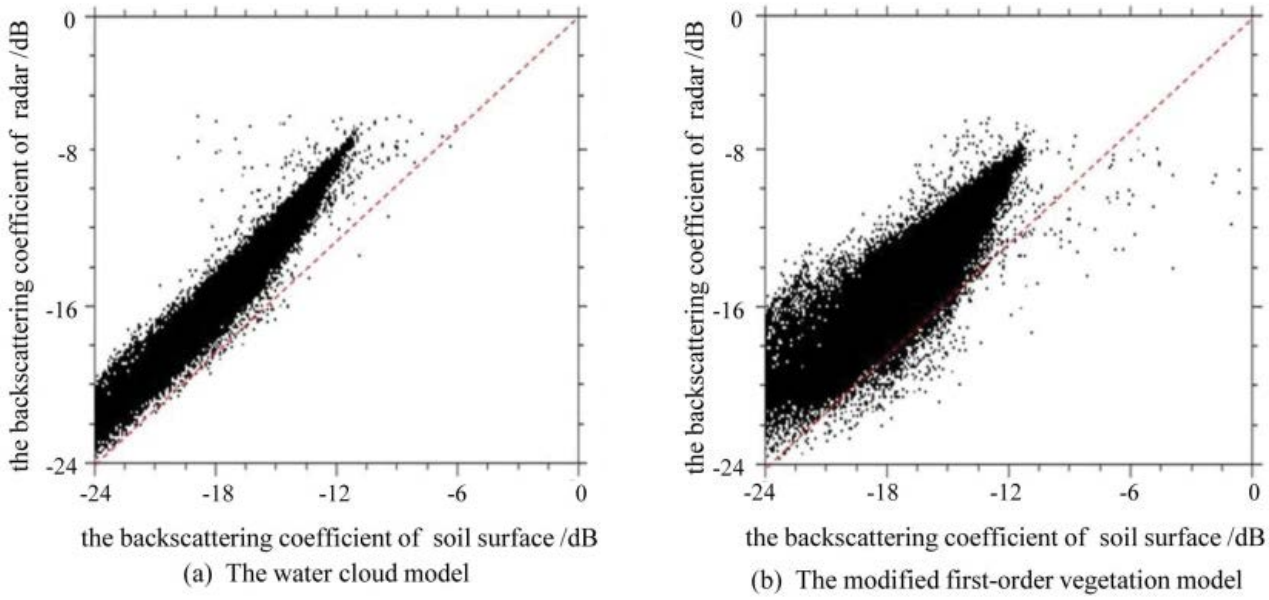

Fig. 6. Comparing the simulation results from different models. (a) The relationship between the soil backscattering coefficient and the total radar backscattering coefficient for the water cloud model (without cross-scattering). (b) The relationship between the soil backscattering coefficient and the total radar backscattering coefficient for the modified first-order vegetation model.

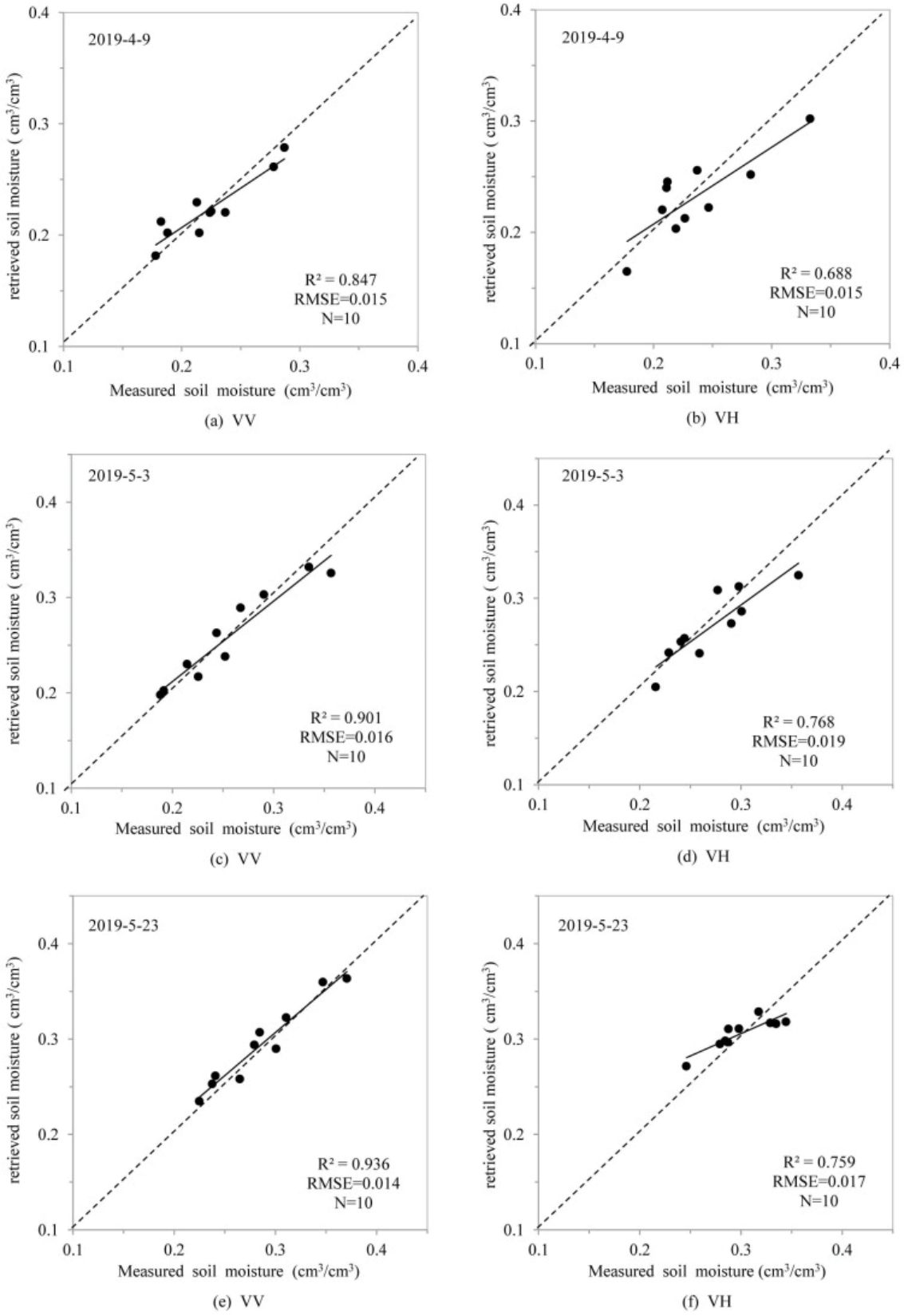

Fig. 7. Comparisons between measured SM values and those retrieved using SVR for different stages of wheat: (a) VV polarization on April 9, 2019, (b) VH polarization on April 9, 2019, (c) VV polarization on May 3, 2019, (d) VH polarization on May 3, 2019, (e) VV polarization on May 23, 2019, and (f) VH polarization on May 23, 2019.

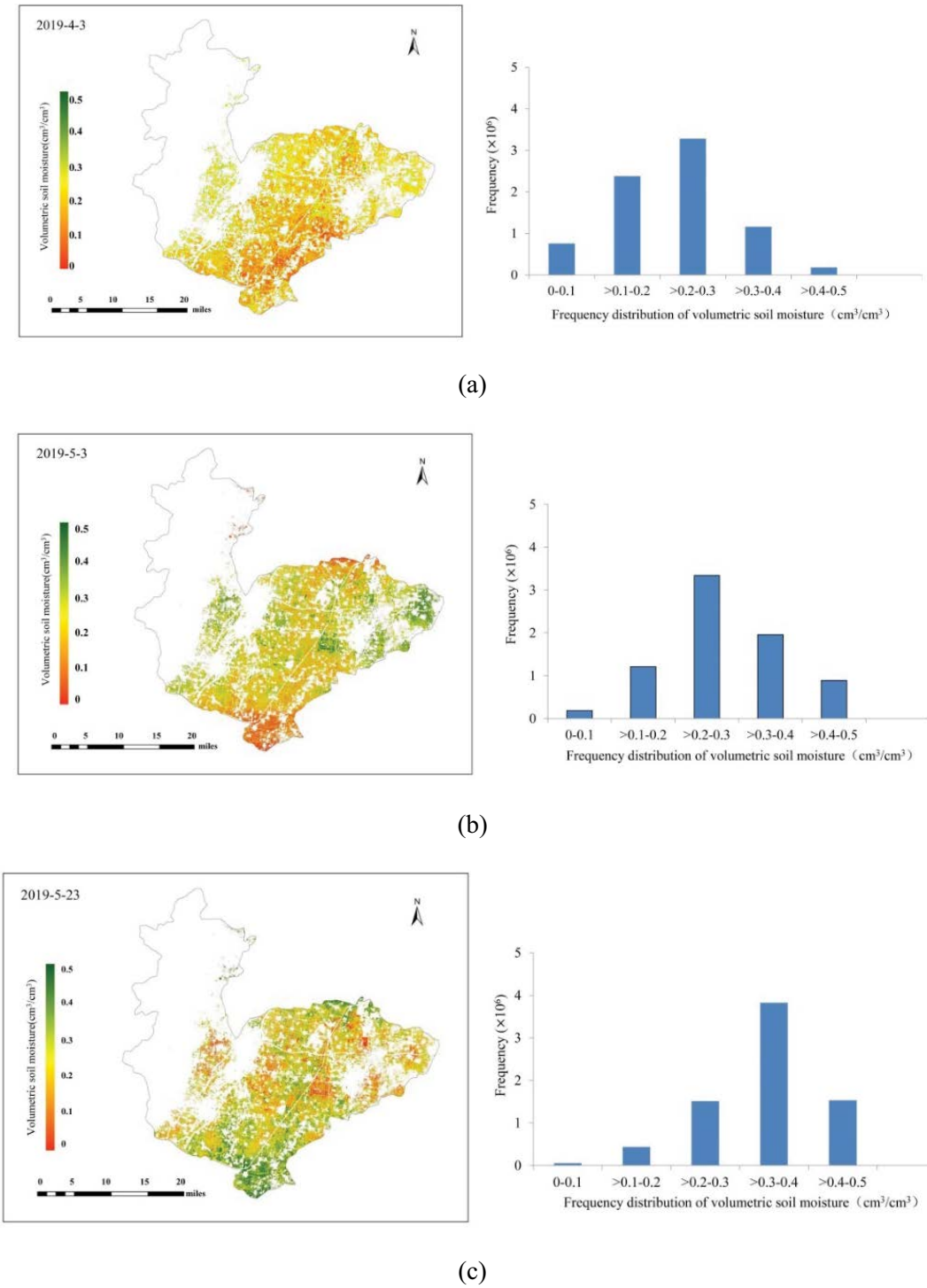

Fig. 8. Spatial distribution of SM retrievals in the study area and frequency diagram of volumetric SM (a) on April 9, 2019; (b) on May 3, 2019; (c) on May 23, 2019.

regarding wheat fields. To extract the soil backscattering coefficient from the radar backscattering coefficient, first a first-order vegetation model was selected and modified. Then, the SM of wheat-covered fields in different periods of growth were retrieved and analyzed under different polarization modes (VV, VH) based on the SVR algorithms. The main conclusions of this study can be summarized as follows:

- With the dual-polarization Sentinel-1 SAR data, the improved first-order vegetation model can decomposed the backscattering related to vegetation and surface from

Table 1
Summary of training and validation results of the SVR for each dataset

	Water cloud model				Modified first-order vegetation model			
	VV		VH		VV		VH	
Time	R^2	RMSE (cm^3/cm^3)	R^2	RMSE (cm^3/cm^3)	R^2	RMSE (cm^3/cm^3)	R^2	RMSE (cm^3/cm^3)
2019-4-3	0.779	0.024	0.491	0.029	0.847	0.015	0.688	0.015
2019-5-3	0.843	0.023	0.658	0.026	0.901	0.016	0.769	0.019
2019-5-23	0.847	0.017	0.580	0.026	0.936	0.014	0.759	0.017

the radar backscattering signals. The results show that this model is better than the water cloud model in removing the influence of vegetation scattering.

- Compared with the performances of the Sentinel-1 VV polarization and VH polarization data in SM estimation, VV polarization data obtain a higher estimation accuracy regarding the SM retrieval. This result also confirms that the VV polarization has more soil backscattering information and is more sensitive to the change of SM than VH polarization.
- In this study, results show that the retrieval SM based on the SAR data are applicable to agricultural environments for wheat. More different sensors, such as L-band ALOS-2 or C-band GF3 may be used to improve the ability to retrieve SM.

Acknowledgements

This work was supported by the State Key Program of National Natural Science of China, grant number 51739009, and by the Open Research Fund project of Henan Key Open Laboratory of Agricultural Meteorological Support and Applied Technology, grant number AMF201807, and the Water Conservancy Science and Technology Project of Henan Province, grant number GG201902, and the Training plan for Young Core Teachers in Colleges of Henan Province, grant number 2019gzgg073.

References

[1] H. Vereecken, J.A. Huisman, H.J. Hendricks Franssen, N. Brüggemann, H.R. Bogena, S. Kollet, M. Javaux, J. van der Kruk, J. Vanderborght, Soil hydrology: recent methodological advances, challenges, and perspectives, Water Resour. Res., 51 (2015) 2616–2633.
[2] J. Wang, J.-L. Ding, W.-Q. Chen, A.-X. Yang, Microwave modeling of soil moisture in Oasis regional scale based on Sentinel-1 radar images, J. Infrared Millimeter Waves, 36 (2017) 120–126.
[3] X. Bai, L. Zhang, C. He, Y. Zhu, Estimating regional soil moisture distribution based on NDVI and land surface temperature time series data in the upstream of the Heihe River watershed, Northwest China, Remote Sens., 12 (2020) 2414, doi: 10.3390/rs12152414.
[4] L. Brocca, T. Tullo, F. Melone, T. Moramarco, R. Morbidelli, Catchment scale soil moisture spatial–temporal variability, J. Hydrol., 422 (2012) 63–75.
[5] J. Dong, W.T. Crow, K.J. Tobin, M.H. Cosh, D.D. Bosch, P.J. Starks, M. Seyfried, C. Holifield Collins, Comparison of microwave remote sensing and land surface modeling for surface soil moisture climatology estimation, Remote Sens. Environ., 242 (2020) 111756, doi: 10.1016/j.rse.2020.111756.
[6] M. Aubert, N.N. Baghdadi, M. Zribi, K. Ose, M. El Hajj, E. Vaudour, E. Gonzalez-Sosa, Toward an operational bare soil moisture mapping using TerraSAR-X data acquired over agricultural areas, IEEE J. Sel. Top. Appl. Earth Obs. Remote Sens., 6 (2013) 900–916.
[7] J. Guo, J. Liu, J. Ning, et al., Construction and validation of soil moisture retrieval model in farmland based on Sentinel multi-source data, Trans. Chin. Soc. Agric. Eng., 35 (2019) 71–78.
[8] D.D. Alexakis, F.-D.K. Mexis, A.-E.K. Vozinaki, I.N. Daliakopoulos, I.K. Tsanis, Soil moisture content estimation based on Sentinel-1 and auxiliary earth observation products. A hydrological approach, Sensors, 17 (2017) 1455–1461.
[9] X.J. Zeng, Y.Q. Xing, W. Shan, Y. Zhang, C.Q. Wang, Soil water content retrieval based on Sentinel-1A and Landsat 8 image for Bei'an-Heihe expressway, Chin. J. Eco-Agric., 25 (2017) 118–126.
[10] M.I. Sancer, Shadow-corrected electromagnetic scattering from a randomly rough surface, IEEE Trans. Antennas Propag., 17 (1969) 577–585.
[11] Q. Zhang, F. Xu, Q. Zou, Inversion of bare soil moisture by the least squares support vector machine approach combined with SPM, Dianbo Kexue Xuebao/Chin. J. Radio Sci., 30 (2015) 300–306.
[12] J. Wang, J.-L. Ding, W.-Q. Chen, A.-X. Yang, Microwave modeling of soil moisture in Oasis regional scale based on Sentinel-1 radar images, J. Infrared Millimeter Waves, 36 (2017) 120–126.
[13] J.L. Kong, J.J. Li, P.P. Zhen, et al., Inversion of soil moisture in arid area based on microwave and optical remote sensing data, J. Geo-Inf. Sci., 18 (2016) 857–863.
[14] M. Zribi, A. Gorrab, N. Baghdadi, Z. Lili-Chabaane; B. Mougenot, Influence of radar frequency on the relationship between bare surface soil moisture vertical profile and radar backscatter, IEEE Geosci. Remote Sens. Lett., 11 (2013) 848–852.
[15] S.-K. Kweon, Y. Oh, Estimation of soil moisture and surface roughness from single-polarized radar data for bare soil surface and comparison with dual- and quad-polarization cases, IEEE Trans. Geosci. Remote Sens., 52 (2014) 4056–4064.
[16] Y.S. Bao, L. Lin, S.Y. Wu, K.A.K. Deng, G.P. Petropoulos, Surface soil moisture retrievals over partially vegetated areas from the synergy of Sentinel-1 and Landsat 8 data using a modified water-cloud model, Int. Appl. Earth Obs. Geo-Inf., 72 (2018) 76–85.
[17] E.P.W. Attema, F.T. Ulaby, Vegetation modeled as a water cloud, Radio Sci., 13 (1978) 357–364.
[18] C. Xun, T. Zhang, S. Yun, H. Gong, L. Liu, K. Xie, Modeling and mapping soil moisture of plateau pasture using RADARSAT-2 imagery, Remote Sens., 7 (2015) 1279–1299.
[19] P.C. Dubois, J. van Zyl, T. Engman, Measuring soil moisture with imaging radars, IEEE Trans. Geosci. Remote Sens., 33 (2002) 915–926.
[20] L.N. Lin, Y. Bao, Q. Zuo, et al., Soil moisture retrieval over vegetated areas based on Sentinel-1 and FY-3C data, Remote Sens. Technol. Appl., 33 (2018) 750–758.
[21] F.T. Ulaby, K. Sarabandi, K. Mcdonald, M. Whitt, M. Craig Dobson, Michigan Microwave Canopy Scattering model, Int. J. Remote Sens., 11 (1990) 1223–1253.
[22] J.B. Jiang, D.H. Hu, Y.Q. Liu, et al., Research of soil moisture retrieval model of wheat covered surface based on MIMICS model, J. Triticeae Crops, 35 (2015) 707–713.

[23] R.D. de Roo, Y. Du, F.T. Ulaby, M.C. Dobson, A semi-empirical backscattering model at L-band and C-band for a soybean canopy with soil moisture inversion, IEEE Trans. Geosci. Remote Sens., 39 (2001) 864–872.
[24] J.C. Shi, J.-S. Lee, K.S. Chen, Q. Sun, Evaluate usage of decomposition technique in estimation of soil moisture with vegetated surface by multi-temporal measurements data, J. Remote Sens., 6 (2002) 412–415.
[25] W. Liu, J.C. Shi, J.M. Wang, Applying the decomposition technique in vegetated surface to estimate soil moisture by multi-temporal measurements, Remote Sens. Inf., 4 (2005) 3–6.
[26] C. Ren, Y.-J. Liang, X.J. Lu, H.-B. Yan, Research on the soil moisture sliding estimation method using the LS-SVM based on multi-satellite fusion, Int. J. Remote Sens., 40 (2019) 2104–2119.
[27] G. Bertoldi, S.D. Chiesa, C. Notarnicola, L. Pasolli, G. Niedrist, U. Tappeiner, Estimation of soil moisture patterns in mountain grasslands by means of SAR RADARSAT2 images and hydrological modeling, J. Hydrol., 516 (2014) 245–257.
[28] J.S. Lee, L. Jurkevich, P. Dewaele, P. Wambacq, Speckle filtering of synthetic aperture radar images: a review, Remote Sens. Rev., 8 (1994) 313–340.
[29] G. Garcia-Ros, I. Alhama, F. Alhama, Dimensionless characterization of the non-linear soil consolidation problem of Davis and Raymond. Extended models and universal curves, Appl. Math. Nonlinear Sci., 4 (2019) 61–78.
[30] C. Ogwah, M.O. Eyankware, Investigation of hydrogeochemical processes in groundwater resources located around abandoned Okpara Coal Mine, Enugu Se. Nigeria, J. Clean WAS, 4 (2020) 12–16.
[31] B. Singh, P. Sihag, A. Parsaie, A. Angelaki, Comparative analysis of artificial intelligence techniques for the prediction of infiltration process, Geol. Ecol. Landscapes, 5 (2021) 109–118.
[32] M. Pesaresi, C. Corbane, A. Julea, A.J. Florczyk, V. Syrris, P. Soille, Assessment of the added-value of Sentinel-2 for detecting built-up areas, Remote Sens., 8 (2016) 299, doi: 10.3390/rs8040299.
[33] G. Gutman, A. Ignatov, The derivation of the green vegetation fraction from NOAA/AVHRR data for use in numerical weather prediction models, Int. J. Remote Sens., 19 (1998) 1533–1543.
[34] J. Guo, J. Liu, J. Ning, Construction and validation of soil moisture retrieval model in farmland based on Sentinel multi-source data, Trans. Chin. Soc. Agric. Eng., 35 (2019) 71–78.
[35] Y. Oh, Quantitative retrieval of soil moisture content and surface roughness from multipolarized radar observations of bare soil surfaces, IEEE Trans. Geosci. Remote Sens., 42 (2004) 596–601.
[36] K. Zhang, Q. Wang, L. Chao, J. Ye, Z. Li, Z. Yu, T. Yang, Q. Ju, Ground observation-based analysis of soil moisture spatiotemporal variability across a humid to semi-humid transitional zone in China, J. Hydrol. (Amsterdam), 574 (2019) 903–914.
[37] J.H. Zhao, B. Zhang, N. Li, Z. Guo, Cooperative inversion of winter wheat covered surface soil moisture based on Sentinel-1/2 remote sensing data, J. Electron. Inf. Technol., 43 (2021) 692–699.
[38] N. Baghdadi, M. El Hajj, M. Zribi, S. Bousbih, Calibration of the water cloud model at C-Band for winter crop fields and grasslands, Remote Sens., 9 (2018) 969, doi: 10.3390/rs9090969.
[39] K. Zhang, L.-j. Chao, Q.-q. Wang, Y.-c. Huang, R.-h. Liu, Y. Hong, Y. Tu, W. Qu, J.-y. Ye, Using multi-satellite microwave remote sensing observations for retrieval of daily surface soil moisture across China, Water Sci. Eng., 12 (2019) 85–97.
[40] Y. Wang, J. Kong, L. Yang, et al., Remote sensing inversion of soil moisture in vegetation-sparse arid areas based on SVR, J. Geo-Inf. Sci., 21 (2019) 1275–1283.